Archeologia e Calcolatori
34.2, 2023, 207-223
doi 10.19282/ac.34.2.2023.11

MULTISPECTRAL AND HIGH-RESOLUTION IMAGES AS SOURCES FOR ARCHAEOLOGICAL SURVEYS. NEW DATA FROM IRAQI KURDISTAN

1. Introduction

Remote Sensing (RS) is a well-established resource for archaeological research. The first RS applications to archaeology with the first aerial photos were conducted at the end of the 19th century in Europe and during the early decades of the 20th century in the Near East (Poidebard 1934). With the rise of satellite imagery, the remote observation of the ground could be performed at a completely different scale. The relatively low spatial resolution of the first sensors hampered the possibility of identifying small archaeological features but gave an incredible boost to approaching the wider landscape framework and relations between different sites. The availability of commercial satellites equipped with sensors, whose pixel size was less than ten meters, subsequentely also allowed the identification of sites that were previously undetectable. The appearance of multispectral sensors then allowed us to see what was invisible, much more deeply than was possible using analogue infrared films.

The recent fast development of software, data access and artificial intelligence applications are again revolutionizing RS applications for archaeology, with a worldwide impact for the entire discipline (Forte, Campana 2016). The availability of new archival material opened the way to new discoveries as well: the declassification of military data such as the CORONA imagery offered additional resources that are particularly important for landscape archaeology applications, especially in the Near East area, as their acquisition period dates back to the 1960s, before the massive urban development of the second half of the 20th century (Casana, Cothren 2013). Among the most notable advances concerning RS data processing, the most important is cloud computing applied to geospatial products: large datasets containing hundreds of images or other types of data can be processed by users who can rely on cloud infrastructures. This computational power allows analysis at an unprecedented scale. Google Earth Engine (GEE) is a popular and free online resource for geospatial processing (Gorelick *et al.* 2017). GEE can be used to create and analyse RS big data, producing for instance mosaicked images or land use analysis using decades of satellite images. Although the spatial resolution of the available datasets is usually quite low for the immediate identification of small-sized archaeological features on the ground, GEE can be succesfully used to retrieve other useful information, such as the level of moisture in the soil, and to identify the larger sites. Its use is also spreading within the archaeological community with applications in the Near East area such as in Jordan (Liss *et al.* 2017), Syria (Agapiou 2020) and Iraqi Kurdistan as well (Titolo 2021).

During recent decades, archaeological missions in the area of ancient North Mesopotamia, which currently belongs to the Iraqi Kurdistan autonomous region, have increased in number and scope, helping to reveal a known but previously underestimated archaeological heritage. Several international archaeological missions are active in this area; most of them rely on RS as a primary source for site identification and for reconstructing the ancient landscape (Morandi 2016; Pfälzner *et al.* 2016; Kolinski 2018; Ur *et al.* 2021). Other examples of RS applications in Kurdistan have been in the Sulaymaniyah province (Altaweeel, Squitieri 2019), in Erbil province (Soroush *et al.* 2020), the Sirwan region (Laugier, Casana 2021; Laugier *et al.* 2022), on the Kona Makhmūr site (S of Erbil: Starková 2020) as well as in the Navkur Plain (Pirowski *et al.* 2021) and on the Khinis site (Malinverni *et al.* 2017). The last two locations are situated within the area surveyed by the Land of Nineveh Archaeological Project (LoNAP) conducted by the University of Udine since 2012.

R.V.

2. Materials and methods

2.1 *The geomorphological and archaeological landscape*

The Navkur Plain (muddy plain in local Kurmanji Kurdish) covers an area of almost 1400 km². It is characterized by fertile clayey soil, delimited by the Zagros mountain range to the N and E, while the Jebel Bardarash and Jebel Maqloub mountains border it to the W and S, respectively. The plain slopes gently both along the NS and EW axis; it is crossed by several watercourses, most of which are seasonal, with water flowing only during winter and early spring with some exceptions like the Nahr al-Khazir and the Gomel Su, two perennial rivers that deeply cut the plain. The availability of water is guaranteed also by regular rainfall, that ranges between 300 and 600 mm annually, as well as by the several karst springs that occur in the typical hilly landscape of the Zagros foothills (Wirth 1962, abb. 9-10; Forti *et al.* 2021). This variegated landscape therefore offered ideal conditions for human communities that settled in seasonal camps and/or shelters and, since the so-called Neolithic Revolution (c. 10,000 BCE), in permanent settlements. This explains the area's importance for archaeological projects focusing on a number of fundamental themes of the human past, ranging from the study of the Upper Palaeolithic-Neolithic transition to the exploitation of the countryside by large empires that dominated the area in historical periods. Regional survey projects have amply demonstrated the plain's archaeological importance, thanks to the discovery of

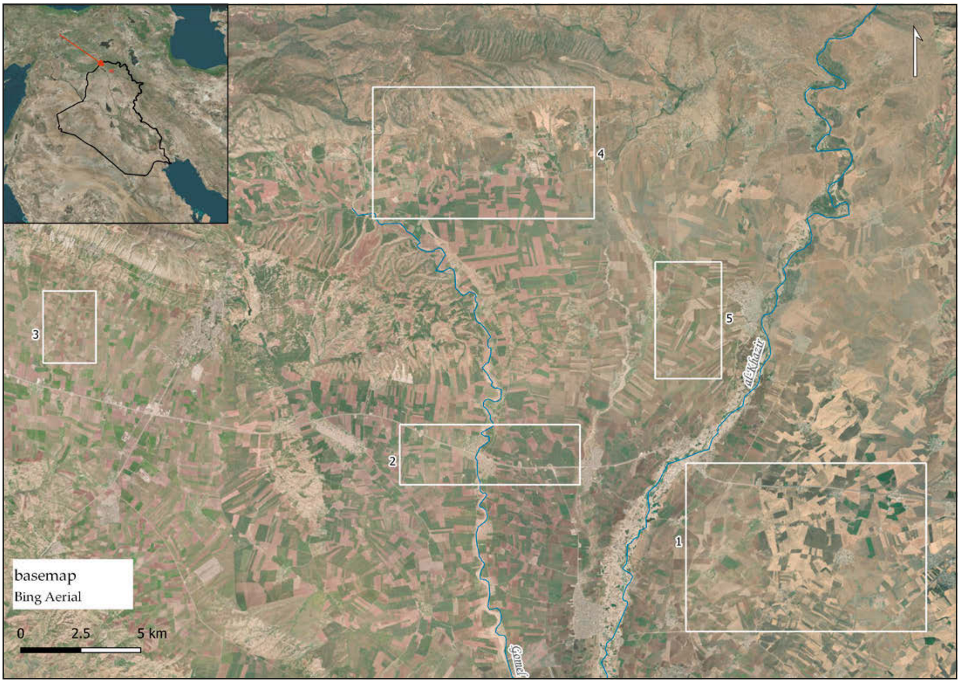

Fig. 1 – Localization of the five surveyed areas in the northern part of Iraq (autonomous Kurdistan region).

a number of settlements dated to prehistoric and historical epochs (Morandi Bonacossi, Iamoni 2015; Koliński 2018). Despite these excellent results, the reconnaissance of the ancient settlements remains a complicated task, in the light of modern settlement and the intensive exploitation of the fertile soils for agricultural purposes. Long settled areas are often more easily recognisable when they pertain to historical epochs. In these cases, the decay of mudbrick structures, such as private houses and public buildings, creates typical mounded sites, known as 'tells' (Arabic) or 'gird' (Kurdish). Settlements characterised by short temporal occupation sequences – the likely consequence of a higher degree of mobility and the associated greater fragility of less permanent housing/residential structures – have given rise to low mounded sites which are less visible in the plain (Wilkinson 2003, 48; Wilkinson, Ur, Hritz 2013, 37-40).

This occurs frequently in prehistoric times, when societies tend to move more easily, but it is also possible that similar phenomena may have taken place in more recent epochs, especially if characterised by socio-political instability. As a result, the investigation of the ancient landscape may miss substantial pieces: in particular, the reconstruction of the earliest phase of human presence, e.g. the Neolithic, when settlements tend to be small and change location over time (Akkermans 2013), may be substantially inaccurate (Nieuwenhuyse, Wilkinson 2008, 271) if adequate methods are not developed to solve these difficulties.

M.I.

2.2 *Target areas (2021-2022)*

Within the larger LoNAP survey area, five smaller target areas (1-5) have been selected for the analysis (Fig. 1): area 1 (about 70 km^2) is close to the Asingeran site and E of the River al-Khazir; area 2 (about 19 km^2) crosses the River Gomel; area 3 (about 7 km^2) is located between 'Baadhrah' and Ash Shaykhan; area 4 (about 50 km^2) covers part of the piedmont area S of the hills that border the Atrush valley to the S; and area 5 (about 13 km^2) is W of the village of Qasrok. They are all situated in the wider Navkur Plain for an overall area of about 159 km^2. The five target areas represent the main morphological characteristics, such as flat regions (3, 4), regions crossing or in between important waterways (2, 5) and regions close to the first high hills that precede the Zagros mountain range (4). While some known sites already surveyed by the LoNAP mission were located in areas 1, 2 and 4, areas 3 and 5 were blank.

R.V.

2.3 *Use of Google Earth Engine for archaeological purposes*

The retrieval and processing of satellite imagery used for this study was carried out with GEE. Within the GEE environment, three main datasets were selected, acquired by three different platforms: Landsat 5 (https://www.usgs.gov/landsat-missions/landsat-5), Landsat 7 (https://www.usgs.gov/landsat-missions/landsat-7) and Sentinel-2 (https://sentinel.esa.int/web/sentinel/missions/sentinel-2). The characteristics of the Landsat multispectral sensors are similar, with an increased spatial resolution for Landsat 7 (Landsat 5: radiometric resolution 0.45-2.35 μm; spatial resolution 30 m reflective, 120 m thermal. Landsat 7: radiometric resolution 0.45-2.35 μm; spatial resolution 15 m panchromatic, 30 m reflective, 60 m thermal). Both of them have seven bands (B1: blue; B2: green; B3: red; B4: near-infrared; B5: short-wave infrared; B6: thermal; B7: mid-infrared), with an additional band (B8: panchromatic) for Landsat 7. Sentinel-2 multispectral sensor is different (radiometric resolution: 0.443-2.19 μm; spatial resolution: from 10 to 60 m) and delivers thirteen bands (B1: ultra blue; B2: blue; B3: green; B4: red; B5- B6- B7- B8: visible and near infrared; B9- B10- B11- B12: short-wave infrared).

An additional dataset (MODIS Combined 16-Days NDWI) acquired by the Terra-Aqua platforms, was used to estimate in the investigated area the

Normalized Difference Water Index (NDWI) value, which shows the quantity of moisture on vegetation and the ground. As archaeological features are usually more visible when the moisture level in the ground is higher, the NDWI trend suggested the selection of images that were acquired within the period January-April, that partially coincides with the 'wet' season in Kurdistan. The average NDWI value was computed for the time interval 2012-2021, that also coincides with the beginning of LoNAP surveys, to assess the trend over a decade.

The added value of GEE is that it is not only an image viewer but also allows for image processing, exploiting the power of cloud computing and making possible computations on large datasets that would otherwise require enormous hardware resources. This allowed the adoption of a multitemporal approach that proved to be particularly efficient for archaeological purposes (Valente *et al.* 2022). Instead of selecting single images from a certain dataset, an entire image stack was chosen within the previously stated seasonal limits. An additional chronological boundary was set: for the Landsat datasets two decades were selected, respectively 1984-1994 for Landsat 5 and 2000-2010 for Landsat 7, while for the more recent Sentinel-2 dataset the chosen interval was 2018-2021. Every stack was further filtered excluding images with high cloud coverage.

The filtered datasets had different composition: 110 images for the Landsat 5 1984-1994 collection, 132 images for the Landsat 7 2000-2010 collection and 31 images for the Sentinel-2 2018-2021 collection. The lower number of images of the last dataset is due to the limited period of acquisition compared to the Landsat collections. Thus, a final output was obtained as the result of a median function applied to every pixel, for each band independently. This way, seasonal visibility of sites was enhanced, limiting constraints due to field conditions such as the presence of crops covering the ground. An additional output was obtained from Sentinel-2 by applying a ratio index ($I_{B4,B8}$= B4/(B4-B8) that uses bands 4 and 8, improving the visibility of anomalies in the image. A pan-sharpening with the panchromatic band was also performed on the Landsat outputs, to increase the spatial resolution from 30 m to 15 m; this operation was not performed on the Sentinel output as the native spatial resolution of some of its bands was already 10 m. All the previous operations were carried out within the GEE interface and through its JavaScript console.

The generated outputs were then uploaded in QGIS to be managed along with the existent spatial data and visualized in false colours to enhance the anomalies that could correspond to unknown archaeological sites. At first, the appearance of known archaeological sites, whose location was stored in a .SHP file, was checked on the new outputs. All the available bands were initially observed: nevertheless, band 5 (that corresponds to shortwave infrared) proved to be more effective with Landsat outputs, while the RGB range,

Fig. 2 – Comparison of archival satellite images of surveyed sites; imagery retrieved using Google Earth Pro.

band 4 (red) and band 8 (near infrared) were found more effective with the Sentinel data. This last output was visualized also with the $I_{B4,B8}$ index applied.

Based on the previous surveys carried out in the same region, the most frequent types of sites in the Navkur Plain are: i) *tells*, i.e., artificial mounds that usually correspond to the principal settlements; ii) flat sites, i.e., sites with no or low elevation, often characterized by lighter coloration of the soil; iii) sites with structures. The latter type can have some variants, spanning from human settlements with remains of residential structures to simple pastoral enclosures. As a general rule, most of the flat sites appear on multispectral satellite images as clearly identifiable neat and round traces, whose colour is different from the surrounding soil; this is due to the different composition of the anthropogenic soil compared to the fertile one. The new visually identified anomalies were recorded in another .SHP files: 42 anomalies were identified in 2021 and 59 in 2022, for a total of 101. This number includes both anomalies that are very similar to the already known sites, and others less evident that would have been subsequently checked on the ground.

The 2022 survey used the same methodology and tools tested in the previous year, increasing however the use of high-resolution imagery freely available through web services such as Google Earth Pro and Bing Maps. These services offer little customization options but share high-resolution images for free, an important aspect when dealing with large areas and limited funds. This way, it was possible to integrate the information coming from the multispectral processed images and the available panchromatic high-resolution images that allow for a better identification of features on the ground. In addition to multispectral images, recent and archival high-resolution imagery was retrieved using Google Earth Pro and compared to observe the identified regions in different images, since their appearance can change substantially depending on the acquisition period (Fig. 2). This approach aimed to verify the limits of the applicability of the previously tested method on the different natural environments of area 4. In fact, in proximity to the rocky hills S of the Zagros mountain range the fertile soil of the plain progressively ends. Due to different environmental conditions, ancient human settlements were more likely to have a different appearance to those in lower lands, or at least to have left different traces in the soil. The first preliminary observations of this area in 2021 on multispectral images revealed less clear results that required a more careful approach.

R.V.

2.4 *Extraction of spectral signatures*

GEE allowed also to extract spectral signatures given a sampling area. The Sentinel-2 median was selected for the spectral signature extraction due to its better spatial resolution. For this study, a 50×50 m sampling area was used for every region corresponding to an identified anomaly: the pixels included within this area were averaged and the corresponding spectral profile was automatically plotted by GEE. As references, also the average spectral signature of areas identified as fields with no archaeological features and the average spectral signature of a selection of known sites were also plotted on the same chart.

R.V.

2.5 *Unsupervised classification and analysis of spectral signatures*

The spectral signatures extracted from the Sentinel-2 dataset were subsequently analysed performing unsupervised statistical classification. Four well-established unsupervised approaches were tested: hierarchical clustering, with the minimum-variance linkage criterion (Ward 1963), k-means (MacQueen 1967), fuzzy c-means (Bezdek 1981) and self-organizing map (SOM) (Kohonen 1982; Maset *et al.* 2015). Classification was performed in Python environment (https://scikit-learn.org/stable/) identifying two clusters. The label for each cluster was then assigned according to its representative element: the one closest to the average spectral signature of already known LoNAP sites represents the 'site' class, whereas the other cluster was identified

Fig. 3 – Localization of surveyed regions over the five areas and results.

as that one containing anomalies with 'no archaeological sites', according to the algorithm. Three datasets were created and separately analysed: spectral signatures of sites surveyed in 2021, in 2022, and a set comprising anomalies detected in both 2021 and 2022, so as to better assess the precise results given the different natural environments of targeted areas.

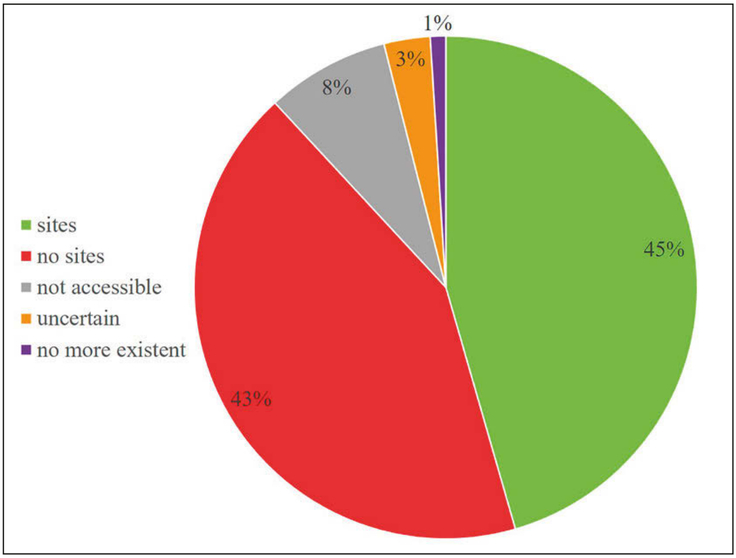

Fig. 4 – Results of 2021-2022 surveys from a total of 101 surveyed regions.

E.M.

2.6 *Ground-truthing assessment*

In order to assess the results of the remote analyses, field surveys were planned. To speed up the fieldwork, the QField app was used to display in real time the position of the team, composed of three to five members, and the locations of the investigated regions (https://qfield.org/). Areas 1, 2 and 3 were surveyed over six days in September and October 2021, while areas 4 and 5 were surveyed over five days in September 2022. In 2022 an additional day was necessary to survey site 426, due to its position on the top of a rocky hill (elevation: 900 m asl). Surface finds, when present, were collected; the subsequent analysis of potsherds also provided preliminary information about the chronology of the surveyed sites, collecting important data for future work on the settlement structure in the Navkur region.

R.V.

3. Results

The 2021-2022 surveys checked on the ground a total number of 101 regions. Eight of these could not be verified because fields were cultivated or because of the presence of fences. Three regions were classified as 'uncertain', because the presence of anthropic material was too scarce to determine a site with confidence, while one single case was a 'disappeared site': a stone enclosure visible in satellite images that had been levelled and only scattered stones were identified on the ground. Forty-three regions did not yield any trace of ancient human presence, while forty-six regions were classified as 'sites' (Fig. 3). The nature of these sites is diverse: two areas were identified as 'ceramic clusters', twelve as *tells*, seventeen as flat sites, four as settlements on rocky hills, five as pastoral structures, five as isolated cemeteries, one as an identified structure (Fig. 4).

With regard to an assessment of the output generated from GEE, both Landsat and Sentinel images gave good results for the identification of new sites. On one hand, Landsat images, that were generated with datasets acquired during the 1985-1995 and 2000-2010 periods, were useful because the landscape they recorded was less urbanized than the contemporary one. On the other, their effectiveness for the identification of new sites was limited by their relatively low spatial resolution. The Sentinel-2 outputs compensated for this constraint with their higher spatial resolution (10 m), allowing identification of smaller sites as well.

A further result achieved by the use of multispectral images is the better identification of site clusters. Potsherds scattered over a large area without any visible discontinuity in their surface distribution are usually related to a single site. This may be true, but the presence of distinct and smaller settlements, indistinguishable with regard to the dispersion of potsherds, may also occur. The use of multispectral images allows better identification of differences in soil, even when these cannot be correctly assessed in the field.

The automatic classification of spectral signatures provided the results summarized in Tab. 1.

Overall, the best performances were reached by k-means and SOM, whereas the hierarchical clustering method appears not to be suitable for this application. Better results were achieved for the 2021 dataset, with a promising overall accuracy of 74% provided by SOM. This corresponds to 12 actual sites correctly identified, and 17 regions that the algorithm correctly classified as 'no site'. On the other hand, performance decreased for the 2022 dataset, with an overall accuracy of 64% achieved by k-means and fuzzy c-means,

	hierarchical clustering	*k-means*	*fuzzy c-means*	SOM
2021	54%	69%	67%	74%
2022	58%	64%	64%	60%
2021 + 2022	53%	60%	57%	57%

Tab. 1 – Overall accuracy provided by the tested algorithms, computed as the ratio of correctly classified sites to the total number of regions analysed.

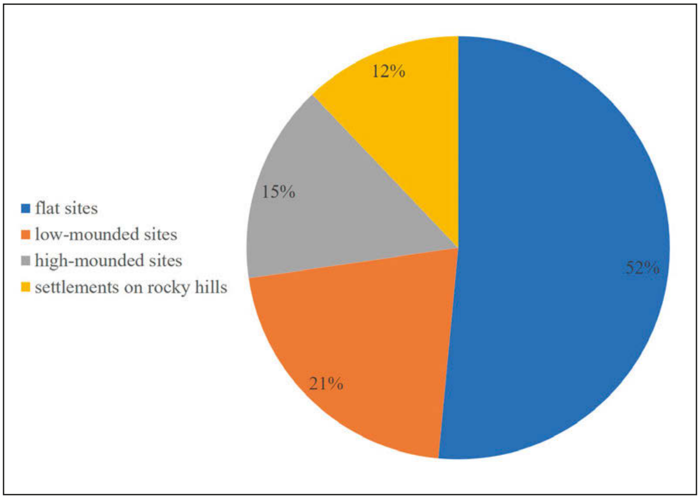

Fig. 5 – Distribution of settlement types among the new sites found: more than half are flat sites on plains, the most difficult type to be detect by RS.

whereas only 60% of the analysed regions were correctly classified by SOM, with 10 actual sites labelled as 'no site' and 10 regions erroneously identified by the algorithm as archaeological sites. No advantages were obtained by jointly processing the spectral signatures of the regions investigated in 2021 and 2022, showing that the different natural environments of the targeted areas affects their spectral signatures, making automatic classification more challenging.

R.V., E.M.

4. Discussion

Most of the new sites (seventeen) identified are flat sites, and this could be expected because sites with elevation are obviously easier to recognize both on RS sources (images but also digital elevation models) and during on-ground surveys. Therefore, most of the sites with elevation had already been discovered in the past LoNAP campaigns. However, the overall number of twelve *tells* identified in 2021 and 2022 is relevant as well: these can be further divided into low-mounded (seven sites) and high-mounded (five sites), depending on their elevation. It is worth noticing that four of five high-mounded tells are located in area 4, and this concentration could be partially explained by the difficult of identifying these sites on the ground in non-plain contexts (Fig. 5).

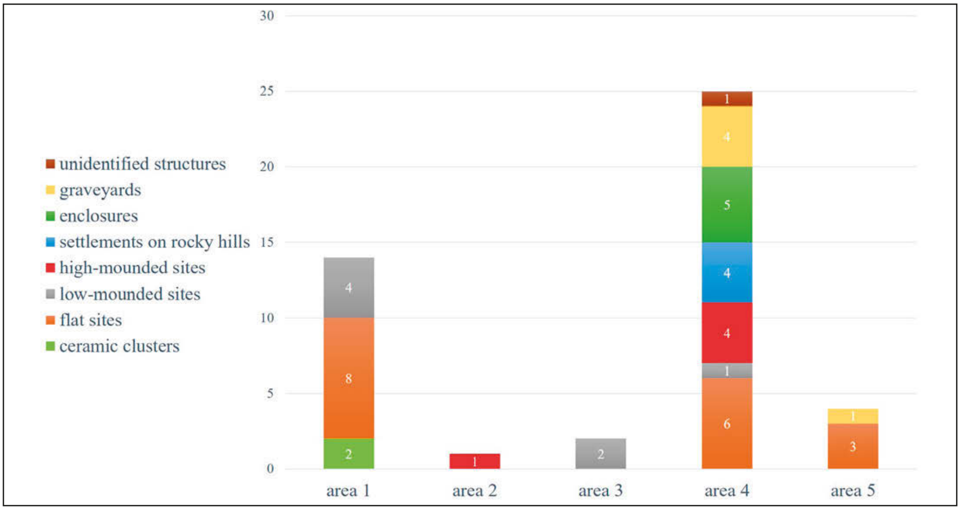

Fig. 6 – Distribution of site types per surveyed area; a marked pre-eminence in number and variety is visible in area 4.

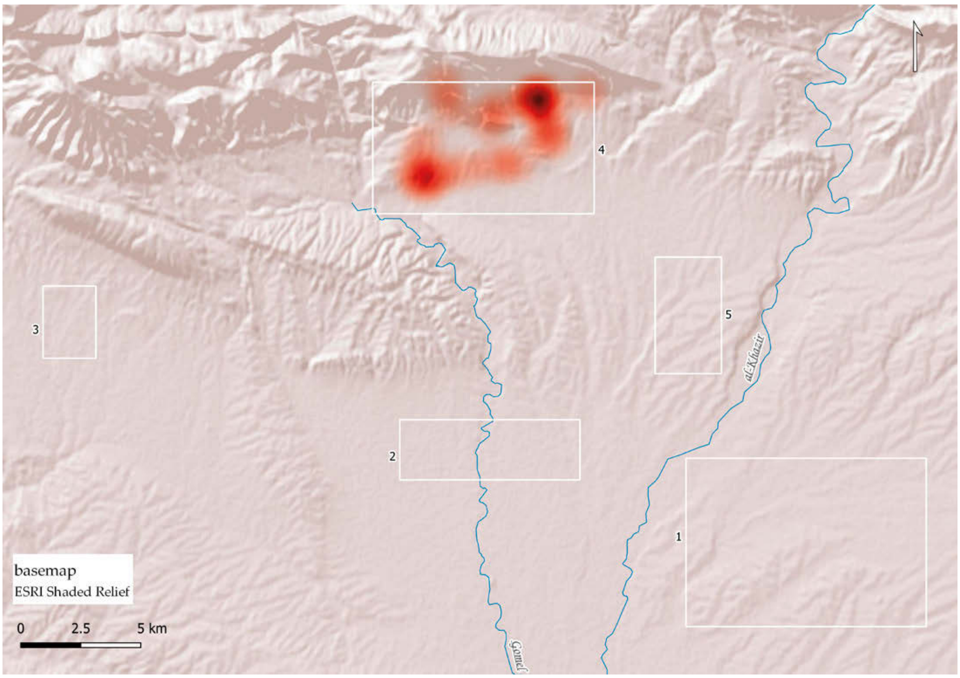

Fig. 7 – Heatmap distribution of new sites with visible remains of standing or collapsed structures; an evident concentration is visible in area 4.

A further analysis of site distribution reveals that area 4, surveyed in 2022, has the highest number of archaeological features (25) followed by area 1, surveyed in 2021, with 14 features; these two areas together yielded the 85% of the overall number of sites found during the two-year survey. Area 4 has also the greatest variety of archaeological features: except for a ceramic cluster, every other type of site was identified (flat sites, low-mounded sites, high-mounded sites, settlements on rocky hills, enclosures, graveyards, unidentified structures) (Fig. 6). This partly depends on the size of the survey area (50 km^2), but also on the peculiarity of this territory at the borders of the Navkur Plain; in comparison in area 1, which is the largest area investigated (70 km^2), only three typologies of sites were found (ceramic clusters, low-mounded and high-mounded sites).

The chronology of the surveyed sites is another noteworthy aspect: they range from the earliest period of stable human presence in the area, i.e., the Pottery Neolithic – c. 7000-4000 BCE – to the most recent one (Ottoman period). This demonstrates the possibility to intercept traces of ancient communities characterized by evanescent archaeological evidence (simple mud architecture) to the most solid remains of ancient buildings with stone walls/structures.

An apparent difference between the 2021 and 2022 field discoveries is that many sites surveyed in 2022 had visible remains of structures variously preserved or pebble heaps, that probably resulted from collapsed structures. Visible structures were located only in sites within area 4, the one closer to the rocky hills (Fig. 7). The morphology distribution of sites with visible structures is very homogeneous: 25% are flat sites, 25% are enclosures, 20% are high-mounded sites and 20% are settlements on hills (the remaining 10% are equally divided between low-mounded sites and the single unidentified structure). Some of these sites yielded a very small number of potsherds, such as sites 411 and 416, despite the many visible structures – suggesting a different nature of the settlements located in the piedmont area compared to those in the plain. A remarkable example is site 399 (Fig. 2): despite the remains of structures clearly visible on a satellite image, accessed via Google Earth Pro and acquired in March 2012, the presence on the ground of heaps of pebbles and the classification of its spectral signature as a true positive, no surface finds were individuated. In this particular case it was considered a site, i.e. a location with past human traces, in view of the remains visible on the archival satellite image, but its chronology remains uncertain. Although the presence of surface potsherds is normally connected with settlements or ceramic clusters, pottery fragments have also been found in proximity of two enclosures (sites 426 and 428) and a graveyard (site 249) that is likely to be a *tell* later converted into a burial place.

The combined use of medium resolution multispectral images and high-resolution panchromatic images was successful, in particular with regard to the piedmont area because of a higher presence of visible structures on the ground and the different composition of soil compared to the fertile land of the plain. The use of high-resolution images is less crucial in relatively flat and cultivated contexts, because most of the flat sites do not show any visible permanent features except for a different colour, whose visibility depends on the surface conditions. On the contrary, they are fundamental where the soil differences are not clearly distinguishable and where surface remains are still preserved; a number of sites surveyed in 2022 were preliminarily identified only on high-resolution panchromatic images, since they were not clear on multispectral images.

While the analysis of spectral signatures proved to be very effective within the plain, its application in the piedmont area revealed some constraints that must be taken into account to correctly interpret the results. Some settlements or structures are located in places where the amount of fertile soil is very low or nearly zero. Moreover, the steep profile prevented any significant accumulation of anthropogenic soil because of natural erosion. For the extraction of spectral signatures, the method presented here uses a sampling area of 50×50 m that works well with the flat sites of the plain, because the frequent morphology of distribution of anthropogenic soil is circular, with a central core that gradually fades outward. When the sample area is centred on the core, most of the pixels that are included within the area cover anthropogenic soil. On the contrary, in hilly contexts most of the sampled soil is natural, partly because of the already mentioned sedimentary process and partly because of the differences in the nature of settlements. Preliminary analysis suggests that settlements here had a scattered distribution of structures rather than a central core; this is due to the fact that inhabitants had to adapt to the different environment, taking advantage of those areas where building was easier. In this challenging context, the future use of a more sophisticated artificial intelligence algorithm for analysis of the multispectral images and the spectral signatures could possibly bring further advantages.

R.V., E.M., M.I.

5. Conclusions

The two-year testing of the use of RS sources and cloud computing tools for the identification of new archaeological sites in the area of the Navkur Plain has yielded interesting results. An overall number of 46 new sites (considering also two ceramic clusters) was found using RS sources within an already surveyed area, proving the advantages of the application of these methods also to areas where archaeological sites are already known. The better spatial resolution of Sentinel-2 than Landsat datasets allowed us to use its products to identify also small and medium-sized ancient settlements that are hardly visible on Landsat images. Small isolated archaeological features still require the use of high-resolution or aerial images, but RS-based archaeological surveys can rely on multispectral medium-resolution imagery for the identification of new settlements. The presented method was successfully tested on both plain and piedmont areas. On rocky hills, or generally when the presence of fertile and anthropogenic soil decreases, high-resolution images are still crucial in order to identify archaeological features.

R.V., E.M., M.I.

Riccardo Valente, Marco Iamoni, Eleonora Maset
Dipartimento di Studi Umanisitici e del Patrimonio Culturale
Università degli Studi di Udine
riccardo.valente@uniud.it, marco.iamoni@uniud.it, eleonora.maset@uniud.it

Acknowledgements

The authors wish to thank the General Directorate of Kurdish Antiquities and the Directorate of Antiquities of Dohuk for their support; the Land of Nineveh Archaeological Project Team for their cooperation; Ylenia Borgonovo, Icaro Bortoluzzi and Francesco Venturoso who participated in the field survey; Francesca Simi for her help and advice. This research was funded by the Università degli Studi di Udine, the Italian Ministry of Foreign Affairs and International Cooperation (MAECI) and the Italian Ministry of University and Research (MUR).

REFERENCES

Agapiou A. 2020, *Detecting looting activity through earth observation multi-temporal analysis over the archaeological site of Apamea (Syria) during 2011-2012*, «Journal of Computer Applications in Archaeology», 3, 1, 219-237.

Akkermans P.M.M.G. 2013, *Living space. Temporality and community segmentation: Interpreting Late Neolithic settlement in Northern Syria*, in O.P. Nieuwenhuyse, R. Bernbeck, P.M.M.G. Akkermans, J. Rogasch (eds.), *The Late Neolithic of Upper Mesopotamia*, Turnhout, Brepols, 63-75.

Altaweel M., Squitieri A. 2019, *Finding a relatively flat archaeological site with minimal ceramics: A case study from Iraqi Kurdistan*, «Journal of Field Archaeology», 44, 8, 523-537.

Bezdek J.C. 1981, *Pattern Recognition with Fuzzy Objective Function Algorithms*, New York-London, Plenum Press.

Casana J., Cothren J. 2013, *The CORONA Atlas Project: Orthorectification of CORONA satellite imagery and regional-scale archaeological exploration in the Near East*, in D.C. Comer, M.J. Harrower (eds.), *Mapping Archaeological Landscapes from Space*, New York, Springer, 33-43.

Forte M., Campana S. 2016, *Digital Methods and Remote Sensing in Archaeology. Archaeology in the Age of Sensing*, Springer, Cham.

Forti L., Perego A., Brandolini F., Mariani G.S., Zebari M., Nicoli K., Regattieri E., Barbaro C.C., Bonacossi D.M., Qasim H.A., Cremaschi M., Zerboni A. 2021, *Geomorphology of the North-Western Kurdistan region of Iraq: Landscapes of the Zagros Mountains drained by the Tigris and Great Zab Rivers*, «Journal of Maps», 17, 2, 225-236.

Gorelick N., Hancher M., Dixon M., Ilyushchenko S., Thau D., Moore R. 2017, *Google Earth Engine: Planetary-scale geospatial analysis for everyone*, «Remote Sensing of Environment», 202, 18-27 (https://linkinghub.elsevier.com/retrieve/pii/S0034425717302900).

Iamoni M., Qasim H.A. 2021, *Asingeran, a Neolithic and Chalcolithic "Iceberg" in Northern Mesopotamia*, «Origini», 43, 9-34.

Kohonen T. 1982, *Self-organized formation of topologically correct feature maps*, «Biological Cybernetics», 43, 1, 59-69.

Kolinski R. 2018, *An archaeological reconnaissance in the Greater Zab Area of the Iraqi Kurdistan (UGZAR) 2012-2015*, in R. Salisbury, R.B. Salisbury, F. Höflmayer, T. Bürge (eds.), *Proceedings of the 10th International Congress on the Archaeology of the Ancient Near East; Volume 2: Prehistoric and Historical Landscapes & Settlement Patterns (Wien 2016)*, Wiesbaden, Harrassowitz Verlag, 13-26.

Laugier E.J., Abdullatif N., Glatz C. 2022, *Embedding the remote sensing monitoring of archaeological site damage at the local level: Results from the "Archaeological practice and heritage protection in the Kurdistan Region of Iraq" project*, «PLOS ONE», 17, 6, e0269796 (https://doi.org/10.1371/journal.pone.0269796).

Laugier E.J., Casana J. 2021, *Integrating satellite, UAV, and ground-based remote sensing in archaeology: An exploration of pre-modern land use in Northeastern Iraq*, «Remote Sensing», 13, 24, 5119 (https://www.mdpi.com/2072-4292/13/24/5119).

Liss B., Howland M.D., Levy T.E. 2017, *Testing Google Earth engine for the automatic identification and vectorization of archaeological features: A case study from Faynan, Jordan*, «Journal of Archaeological Science: Reports», 15, 299-304 (https://linkinghub.elsevier.com/retrieve/pii/S2352409X16308082).

MacQueen J. 1967, *Some methods for classification and analysis of multivariate observations*, in L.M. Le Cam, J. Neyman (eds.), *Proceedings of the Fifth Berkley Symposium on Mathematical Statistics and Probability*, 1, Berkeley, University of California, 281-297.

Malinverni E.S., Pierdicca R., Bozzi C.A., Colosi F., Orazi R. 2017, *Analysis and processing of Nadir and Stereo VHR Pleiadés images for 3D mapping and planning the land of Nineveh, Iraqi Kurdistan*, «Geosciences», 7, 80 (https://doi.org/10.3390/geosciences7030080).

Maset E., Carniel R., Crosilla F. 2015, *Unsupervised classification of raw full-waveform airborne lidar data by self organizing maps*, in V. Murino, E. Puppo (eds.), *Image Analysis and Processing - ICIAP 2015 (Genoa 2015)*, Springer, Cham, 69-72 (https://doi.org/10.1007/978-3-319-23231-7_6).

Morandi Bonacossi D. 2016, *The Land of Niniveh Archaeological Project. Assyrian settlement in the Niniveh hinterland: A view from the centre*, in J. MacGinnis, D. Wicke, T. Greenfield (eds.), *The Provincial Archaeology of the Assyrian Empire*, Cambridge, McDonald Institute for Archaeological Research, 141-150.

Morandi Bonacossi D., Iamoni M. 2015, *Landscape and settlement in the Eastern Upper Iraqi Tigris and Navkur Plains (Northern Kurdistan Region, Iraq). The land of Nineveh archaeological project, seasons 2012-2013*, «Iraq», 77, 9-39 (https://doi.org/10.1017/irq.2015.5).

Nieuwenhuyse O.P., Wilkinson T.J. 2008, *Late Neolithic settlement in the area of Tell Beydar (NE Syria)*, in M. Lebeau, A. Suleiman (eds.), *Beydar Studies* I, Subartu XXI, Turnhout, Brepols, 267-304.

Pfälzner P., Sconzo P., Beutelscheiss R., Edmonds A., Glissmann B., Herdt S., Herrmann J.T., Heydari-Guran S., Kohler J., Mueller Weiner M., Puljiz I., Sharp M. 2016, *The Eastern Habur archaeological survey in Iraqi Kurdistan. A preliminary report on the 2014 season*, «Zeitschrift Für Orient-Archäologie», 9, 10-69.

Pirowski T., Marciak M., Sobiech M. 2021, *Potentialities and limitations of research on VHRS data: Alexander the Great's military camp at Gaugamela on the Navkur Plain in Kurdish Iraq as a test case*, «Remote Sensing», 13, 5, 904 (https://www.mdpi.com/2072-4292/13/5/904).

Poidebard R.P.A. 1934, *La trace de Rome dans le désert de Syrie. Le limes de Trajan a la conquéte arabe. Recherches aériennes (1925-1932)*, Paris.

Soroush M., Mehrtash A., Khazraee E., Ur J.A. 2020, *Deep learning in archaeological remote sensing: Automated qanat detection in the Kurdistan Region of Iraq*, «Remote Sensing», 12, 3, 500 (https://www.mdpi.com/2072-4292/12/3/500).

Starková L. 2020, *Toward a high-definition remote sensing approach to the study of deserted medieval cities in the Near East*, «Geosciences», 10, 369 (https://doi.org/10.3390/geosciences10090369).

Titolo A. 2021, *Use of time-series NDWI to monitor emerging archaeological sites: Case studies from Iraqi artificial reservoirs*, «Remote Sensing», 13, 4, 786 (https://www.mdpi.com/2072-4292/13/4/786).

Ur J., Babakr N., Palermo R., Creamer P., Soroush M., Ramand S., Nováček K. 2021, *The Erbil Plain Archaeological Survey: Preliminary results, 2012-2020*, «Iraq», 83, 205-243.

Valente R., Maset E., Iamoni M. 2022, *Archaeological site identification from open access multispectral imagery: Cloud computing applications in Northern Kurdistan (Iraq)*, «Archaeological Prospection», 29, 4, 1-17 (https://doi.org/10.1002/arp.1874).

Ward Jr. J.H. 1963, *Hierarchical grouping to optimize an objective function*, «Journal of the American Statistical Association», 58, 301, 236-244.

Wilkinson T. 2003, *Archaeological Landscapes of the Near East*, Tucson, University of Arizona.

Wilkinson T.J., Ur J.A., Hritz C. 2013, *Settlement archaeology of Mesopotamia*, in T.J. Wilkinson, G. McGuire, M. Widell, *Models of Mesopotamian Landscapes. How Small-Scale Processes Contributed to the Growth of Early Civilizations*, BAR International Series 2552, Oxford, Archaeopress, 34-55.

Wirth E. 1962, *Agrargeographie des Irak*, Hamburg.

ABSTRACT

The paper presents the results of a two-year archaeological survey carried out in the Iraqi Kurdistan, namely within the Navkur plain that has been extensively explored by the University of Udine since 2012. The surveys were planned in advance using Remote Sensing products available online and processed with Google Earth Engine, a large-scale cloud computing service specifically designed to process geospatial big data and especially satellite imagery. Images from Landsat 5, Landsat 7 and Sentinel-2 platforms were selected, processed and assessed. After two years, an overall number of 46 new and previously unknown sites have been localized and surveyed, contributing to the knowledge of the past history of this portion of the Kurdistan region and testing the use of Remote Sensing cloud-computing applications in the context of Near Eastern archaeological research.